NACA RM L56L21

NACA

# RESEARCH MEMORANDUM

## ZERO-LIFT DRAG OF A LARGE FUSELAGE CAVITY AND A PARTIALLY SUBMERGED STORE ON A 52.5° SWEPTBACK-WING—BODY CONFIGURATION AS DETERMINED FROM FREE-FLIGHT TESTS AT MACH NUMBERS OF 0.7 TO 1.53

By Sherwood Hoffman

Langley Aeronautical Laboratory
Langley Field, Va.

NATIONAL ADVISORY COMMITTEE
FOR AERONAUTICS

WASHINGTON

February 26, 1957
Declassified February 10, 1959

NATIONAL ADVISORY COMMITTEE FOR AERONAUTICS

RESEARCH MEMORANDUM

# ZERO-LIFT DRAG OF A LARGE FUSELAGE CAVITY AND A PARTIALLY SUBMERGED STORE ON A 52.5° SWEPTBACK-WING—BODY CONFIGURATION AS DETERMINED FROM FREE-FLIGHT TESTS AT MACH NUMBERS OF 0.7 TO 1.53

By Sherwood Hoffman

## SUMMARY

A free-flight investigation of a rocket-propelled model at Mach numbers of 0.7 to 1.53 was conducted to determine the drag at zero lift of a configuration with a large fuselage cavity and partially submerged store. The basic configuration consisted of a 52.5° sweptback-wing—body configuration that had a smooth distribution of normal cross-sectional area at a Mach number of 1.0. The store was a parabola of revolution with a fineness ratio of 8, had three fins, and had a length equal to 40 percent of the fuselage length. The midpoint of the store was located longitudinally at a station corresponding to the 10-percent station of the wing mean aerodynamic chord. The cavity was designed from an impression of the submerged part of the store and was made smooth with fairings and rounded edges.

The cavity reduced the configuration drag above a Mach number of 1.25 and had no unfavorable interference effects at high subsonic speeds. When the store was tested in the cavity, the drag increment was twice as large as the isolated store drag at high subsonic Mach numbers; was equal, near Mach number 1.0; and was 40 percent greater, near a Mach number of 1.35.

## INTRODUCTION

The design of external stores for supersonic airplanes has been greatly enhanced by area-rule analysis and flow-field studies. Previous investigations generally have been limited to relatively small stores (that is, fuel tanks, bombs, and nacelles) for locations on wings. Very large stores seemed to be out of the question, especially for airplanes having thin and low-aspect-ratio wings. A possible solution to this

problem would be underfuselage stores, either partially submerged in a cavity or exposed. Partially submerged stores (ref. 1) and missiles (ref. 2) can be located to give tolerable drag penalties. When a store is dropped to expose the cavity, however, the cavity drag may vary up to three times that of the partially submerged store (ref. 1). It is evident that more attention has to be given to the design and location of fuselage cavities if such installations are to become practical for large stores.

The present paper presents the zero-lift drag of a fuselage cavity for a large partially submerged store in the fuselage of a 52.5° sweptback-wing—body combination. The fuselage of the combination was indented symmetrically to cancel only the exposed-wing areas at a Mach number of 1.0. The store had a length equal to 40 percent of the fuselage length, a fineness ratio of 8.0, and three fins. The store and cavity were located in the region of the fuselage indentation where some favorable interference effects were expected from the wing-fuselage flow field. The midpoint location of the store corresponded to the 10-percent station of the wing mean aerodynamic chord. All the configurations were rocket-propelled zero-lift models and were tested at the Langley Pilotless Aircraft Research Station at Wallops Island, Va. The flight tests covered continuous ranges of Mach number varying between Mach numbers of 0.7 and 1.53 with corresponding Reynolds numbers from about $4 \times 10^6$ to $13 \times 10^6$, based on wing mean aerodynamic chord.

## SYMBOLS

| | |
|---|---|
| $A$ | cross-sectional area, sq ft |
| $a$ | tangential acceleration, ft/sec$^2$ |
| $C_D$ | total drag coefficient based on $S_W$ |
| $C_{D_S}$ | store drag coefficient based on $S_F$ |
| $C_{D_f}$ | friction drag coefficient based on $S_W$ or $S_F$ |
| $\bar{c}$ | mean aerodynamic chord of wing, 1.293 ft |
| $g$ | acceleration due to gravity, 32.2 ft/sec$^2$ |
| $L$ | length of fuselage, ft |
| $M$ | free-stream Mach number |

| | |
|---|---|
| $q$ | free-stream dynamic pressure, lb/sq ft |
| $R$ | Reynolds number based on $\bar{c}$ |
| $S_W$ | total plan-form area of wing, sq ft |
| $S_F$ | maximum cross-sectional area of store, sq ft |
| $W$ | weight of model, lb |
| $x$ | station measured from fuselage nose, ft |
| $\gamma$ | angle between flight path and horizontal, deg |

## MODELS

Details and dimensions of the models tested are given in figure 1 and tables I to IV. The normal cross-sectional-area distributions and photographs of the models are presented in figures 2 and 3, respectively.

The basic configuration, model A, was used originally as part of the investigation of reference 3 and consisted of a sweptback wing mounted on an indented fuselage with four stabilizing fins. The fuselage first was formed from two parabolas of revolution joined at the maximum diameter station (40 percent of body length) and then was indented symmetrically to cancel the exposed-wing cross-sectional areas normal to the axis of symmetry. The resultant wing-body area distribution or Mach number 1.0 area distribution was smooth and corresponded to that of the original fuselage alone. The overall fineness ratio of the fuselage before and after indenting was 10.0. The wing had an angle of sweepback of 52.5° along the quarter-chord line, an aspect ratio of 3.0 (based on total wing plan-form area), a taper ratio of 0.2, and an NACA 65A004 airfoil section in the free-stream direction. The wing plane passed through the fuselage center line, and the quarter-chord point of the mean aerodynamic chord was located longitudinally at the 60-percent fuselage station. The ratio of total wing plan-form area to body frontal area was 16.5. The stabilizing fins were swept back 60° along the leading edge, had sharp leading and trailing edges, and were interdigitated 45° from the wing plane. The models were constructed mostly from mahogany and aluminum alloys as may be seen in figure 3. The fuselage nose was made from solid brass.

Model B consisted of the basic configuration with a partially submerged parabolic store in the bottom of the fuselage (fig. 1(b)). The store had a fineness ratio of 8, a length equal to 40 percent of the fuselage length, and three equally spaced fins. The store was positioned longitudinally with its midpoint at a station corresponding to the

10-percent station of the wing mean aerodynamic chord. The store axis was made parallel to the fuselage center line and the store was rotated to fit one of the fins into a vertical slot in the body. For the present design, the vertical displacement was determined by submerging the pointed store nose just below the fuselage surface. A smooth cavity was formed from an impression of the submerged part of the store by using smooth fairings and by rounding off the sharp edges of the cavity. The cavity reduced the fuselage volume by 4.5 percent; however, the partially submerged store increased the volume of the original fuselage by approximately 11 percent. Model C was the configuration with the cavity exposed or with the store removed. Model D was a 0.385-scale model of the parabolic store.

## TESTS AND MEASUREMENTS

All the models were tested at the Langley Pilotless Aircraft Research Station at Wallops Island, Va. Models A to C were boosted from zero-length launchers by fin-stabilized 6-inch ABL Deacon rocket motors (fig. 3(e)) to supersonic speeds. After burnout of the rocket motors, the boosters drag-separated from the models and the models decelerated through the test Mach number range. The isolated store, model D, was propelled to supersonic speeds from a helium gun which is described in reference 4. Velocity and trajectory data were obtained from the CW Doppler velocimeter and the NACA modified SCR 584 tracking radar unit, respectively. A survey of atmospheric conditions including winds aloft was made by rawinsonde measurements from an ascending balloon that was released at the time of each launching.

The rocket-propelled models covered continuous ranges of Mach number varying between Mach numbers 0.7 and 1.53. The corresponding Reynolds numbers varied from approximately $4 \times 10^6$ to $13 \times 10^6$, based on wing mean aerodynamic chord, as is shown in figure 4. Model D covered a range of Mach numbers from 0.84 to 1.35 with corresponding Reynolds number range from about $3 \times 10^6$ to $5 \times 10^6$ (fig. 4), based on scaled-down mean aerodynamic chord of the wing. The values of total drag coefficient, based on total wing plan-form area, were obtained during decelerating flight from the expression:

$$C_D = -\frac{W}{qgS_w}(a + g \sin \gamma)$$

where $a$ was obtained by differentiating the velocity-time curve from the CW Doppler velocimeter. The values of $q$ and $\gamma$ were determined from the measurements of tangential velocity and atmospheric conditions along

the trajectory of each model. The error in total drag coefficient was estimated to be less than ±0.0007 at supersonic speeds and ±0.001 at subsonic speeds. The Mach numbers were determined within ±0.01 throughout the test range.

The pressure drag or drag rise coefficient was obtained by subtracting the friction drag from the total drag coefficient for each model tested. The friction drag coefficient at supersonic speeds was estimated by adjusting the subsonic drag level for Reynolds number and Mach number effects by using Van Driest's turbulent-friction coefficients for flat plates (ref. 5). The pressure drag was not corrected for base-drag rise; however, reference 6 and unpublished data indicate that the base-drag rise would be small and of the order of 0.001 when based on wing area.

## RESULTS

### Basic Data

The basic drag data for the models are presented in figure 5. The solid curves are fairings through the measured total drag coefficients. All the models were flight tested at zero-lift or near zero-lift conditions. The data from models A and D, which were symmetrical configurations, are at zero lift. Models B and C were unsymmetrical to the degree of adding the partially submerged store and the cavity, respectively. The centers of gravity of these models were located to give static margins greater than one mean aerodynamic chord length; this condition resulted in very low trim lift coefficients where the induced drag is negligible. The dashed curves are the computed friction drag coefficients through the Reynolds number and Mach number ranges of the tests. Although the isolated store (model D) was smaller than the one used on configuration B, its friction drag and total drag coefficients are equally valid for the larger store. The difference in store skin-friction drag coefficient due to changing scale and Reynolds number is less than the accuracy of the drag measurements.

### Total Drag

The variations of total drag coefficient with Mach number are compared in figure 6(a). The store-plus-interference drag is the increment in $C_D$ of model B over model C. At supersonic speeds, the incremental drag increases from a value equal to the isolated store drag near $M = 1.0$ to about 40 percent more drag than the isolated store near $M = 1.35$. Near $M = 0.90$, the incremental drag is approximately twice the subsonic drag of the isolated store. About half of this subsonic increment can be accounted for by the store friction drag. The other half appears to be

due to pressure interference and experimental errors. The gradual rise in $C_D$ for model B starting near $M = 0.8$ indicates the unfavorable interference between the store, fuselage, and wing at high subsonic Mach numbers. It is possible that this increment may be reduced by a more meticulous design in the region of the store afterbody and fuselage.

An important result of the present investigation is the favorable drag from the cavity. A comparison of $C_D$ for models A and C in figure 6(a) shows that the cavity lowered the drag of the basic configuration (or configuration with cavity closed) above $M = 1.25$ and had no unfavorable interference effects at high subsonic speeds. At transonic speeds, the drag increment due to the cavity is less than half the drag of the isolated store. In the cavity-fuselage (no wings) investigation of reference 1, the cavities tested were impressions of a semi-submerged store in three longitudinal positions and had no edge fairings or radii. The drags from the referenced cavities were either equal to or greater than the drag of their isolated store throughout the Mach number range. It appears that the low-drag cavity design achieved herein was due largely to such factors as favorable pressure interference from the combined fuselage-wing pressure fields acting about the cavity and, also, the cavity fairings which effectively reduced the local peak velocities along the cavity edges. In regard to the flow-field interference, reference 7 shows that it is possible to estimate whether the interference would be favorable at supersonic speeds from an elementary knowledge of the surrounding flow fields. For example, the positive pressure coefficients from the wing leading edge acting on the forward part of the cavity and the negative pressure coefficients from the midchord part of the wing acting on the rear half of the cavity would be expected to produce a thrusting force. If the cavity is assumed to be in the pressure field of the basic fuselage, the interference pressure coefficients would be negative throughout the cavity. Thus, a drag force would be obtained at the forward part of the cavity and a thrust force, at the rear part of the cavity. The overall effects indicate favorable interference for the cavity. Since the store-body slopes are of opposite sign with respect to the cavity and the interference pressure fields are about the same as those about the cavity, the opposite effect or unfavorable interference would be expected for the store in its present location.

## Pressure Drag

The pressure drags of the models are presented in figure 6(b) for comparison with the normal cross-sectional areas shown in figure 2. According to the transonic area rule of reference 8, the zero-lift drag rise (or pressure drag) near $M = 1.0$ is primarily dependent on the rate of development of normal cross-sectional area. When the cavity was cut into the fuselage of the basic configuration, the configuration area distribution was dented to give large changes in slope and a small reduction in maximum cross-sectional area (model C). These changes correspond

to increasing the pressure drag at transonic speeds as may be seen by comparing the results for models C and A in figure 6(b). By installing the store in the cavity (model B), the area slope distribution was altered to give higher slopes and a much greater maximum cross-sectional area than those of either model A or model C. Figure 6(b) shows that model B had the highest transonic pressure drag. The degree to which these changes in area distribution affected the pressure drag cannot be determined from inspection of the area curves. In either case, according to the linearized theory study made of bumps and indentations in reference 9, it can be shown that the pressure drag increases at low supersonic speeds if volume is added or subtracted from a smooth basic configuration as in the manner used herein.

Above $M = 1.3$ the pressure drag increment due to adding the store to the cavity was approximately equal to the isolated store pressure drag; whereas, the increment from the cavity measured with respect to the basic configuration is negative. Although no supersonic area rule (ref. 10) study was made, it seems reasonable that the areas removed by the cavity (in its present location) would subtract from the wing areas cut by oblique Mach planes and, possibly, improve the overall area distribution when the cavity is left open. Hence, it appears that a more rewarding procedure by which reductions in pressure drag could be obtained at supersonic speeds would be to design the cavity configuration specifically for a supersonic Mach number.

## CONCLUDING REMARKS

The present investigation shows that it is possible to design a low drag fuselage cavity for a large partially submerged store or bomb for an airplane. The cavity was designed for an impression of the submerged part of the store; however, it was kept in mind that smooth fairings and round edges would favor low subsonic drag, a fairly smooth normal area distribution would be desirable for low transonic drag rise, and that a favorable wing-body pressure field would have a desirable effect on the interference drag. The results showed that the drag increments from the cavity were negligible at high subsonic speeds, small at transonic speeds, and negative above a Mach number of 1.25. When the store was added to the cavity, the drag increment was approximately twice the value of the

isolated store drag at high subsonic speeds, was equal to the isolated store drag near Mach number 1.0, and was about 40 percent greater than the isolated store drag near a Mach number of 1.35.

Langley Aeronautical Laboratory,
National Advisory Committee for Aeronautics,
Langley Field, Va., December 3, 1956.

REFERENCES

1. Hoffman, Sherwood, and Wolff, Austin L.: Effect on Drag of Longitudinal Positioning of Half-Submerged and Pylon-Mounted Douglas Aircraft Stores on a Fuselage With and Without Cavities Between Mach Numbers 0.9 and 1.8. NACA RM L54E26, 1954.

2. King, Thomas J., Jr.: Wind-Tunnel Investigation at High Subsonic Speeds of Drag at 0° Angle of Attack of Swept-Wing—Fuselage Models With Pylon-Mounted and Semisubmerged Missiles. NACA RM L56G19a, 1956.

3. Hoffman, Sherwood: A Flight Investigation of the Transonic Area Rule for a 52.5° Sweptback Wing-Body Configuration at Mach Numbers Between 0.8 and 1.6. NACA RM L54H13a, 1954.

4. Hall, James Rudyard: Comparison of Free-Flight Measurements of the Zero-Lift Drag Rise of Six Airplane Configurations and Their Equivalent Bodies of Revolution at Transonic Speeds. NACA RM L53J21a, 1954.

5. Van Driest, E. R.: Turbulent Boundary Layer in Compressible Fluids. Jour. Aero. Sci., vol. 18, no. 3, Mar. 1951, pp. 145-160, 216.

6. Morrow, John D., and Nelson, Robert L.: Large-Scale Flight Measurements of Zero-Lift Drag of 10 Wing-Body Configurations at Mach Numbers From 0.8 to 1.6. NACA RM L52D18a, 1953.

7. Smith, Norman F., and Carlson, Harry W.: The Origin and Distribution of Supersonic Store Interference From Measurement of Individual Forces on Several Wing-Fuselage-Store Configurations. I.- Swept-Wing Heavy-Bomber Configuration With Large Store (Nacelle). Lift and Drag; Mach Number, 1.61. NACA RM L55A13a, 1955.

8. Whitcomb, Richard T.: A Study of the Zero-Lift Drag-Rise Characteristics of Wing-Body Combinations Near the Speed of Sound. NACA Rep. 1273, 1956. (Supersedes NACA RM L52H08.)

9. McLean, F. Edward, and Rennemann, Conrad, Jr.: Supersonic Flow Past Nonlifting Bumped and Indented Bodies of Revolution. NACA TN 3744, 1956.

10. Jones, Robert T.: Theory of Wing-Body Drag at Supersonic Speeds. NACA RM A53H18a, 1953.

TABLE I.- COORDINATES OF NACA 65A004 AIRFOIL

[Stations measured from leading edge]

| Station, percent chord | Ordinate, percent chord |
|---|---|
| 0 | 0 |
| .5 | .311 |
| .75 | .378 |
| 1.25 | .481 |
| 2.5 | .656 |
| 5.0 | .877 |
| 7.5 | 1.062 |
| 10 | 1.216 |
| 15 | 1.463 |
| 20 | 1.649 |
| 25 | 1.790 |
| 30 | 1.894 |
| 35 | 1.962 |
| 40 | 1.996 |
| 45 | 1.996 |
| 50 | 1.952 |
| 55 | 1.867 |
| 60 | 1.742 |
| 65 | 1.584 |
| 70 | 1.400 |
| 75 | 1.193 |
| 80 | .966 |
| 85 | .728 |
| 90 | .490 |
| 95 | .249 |
| 100 | .009 |
| L.E. radius: 0.102 percent chord<br>T.E. radius: 0.010 percent chord | |

TABLE II.- COORDINATES OF BASIC FUSELAGE

[Stations measured from body nose]

| Station, in. | Ordinate, in. |
|---|---|
| 0 | 0 |
| 1 | .245 |
| 2 | .481 |
| 4 | .923 |
| 6 | 1.327 |
| 10 | 2.019 |
| 14 | 2.558 |
| 18 | 2.942 |
| 22 | 3.173 |
| 26 | 3.250 |
| 30 | 3.176 |
| 34 | 2.934 |
| 38 | 2.619 |
| 42 | 2.341 |
| 46 | 2.243 |
| 50 | 2.297 |
| 54 | 2.251 |
| 58 | 2.149 |
| 62 | 1.857 |
| 65 | 1.615 |

TABLE III.- COORDINATES OF 26-INCH PARABOLIC STORE[1]

[Stations measured from body nose]

| Station, in. | Ordinate, in. |
|---|---|
| 0 | 0 |
| 1.3 | .309 |
| 2.6 | .585 |
| 5.2 | 1.040 |
| 7.8 | 1.365 |
| 10.4 | 1.560 |
| 13.0 | 1.625 |
| 15.6 | 1.560 |
| 18.2 | 1.365 |
| 20.8 | 1.040 |
| 23.4 | .585 |
| 24.7 | .309 |
| 26.0 | 0 |

[1]Coordinates for the small parabolic store are 0.3846 scale of these coordinates.

TABLE IV.- COORDINATES OF CAVITY[1]

[Stations measured from fuselage nose]

| Stations, in. | $C_r$ | $F_r$ |
|---|---|---|
| 18.00 | 0 | 0 |
| 20.00 | .030 | 1.750 |
| 22.00 | .050 | 1.250 |
| 24.00 | .180 | 1.000 |
| 26.00 | .529 | .625 |
| 28.00 | .901 | .375 |
| 30.00 | 1.196 | .312 |
| 32.00 | 1.415 | .250 |
| 34.00 | 1.556 | .187 |
| 36.00 | 1.620 | .250 |
| 36.67 | 1.625 | .270 |
| 38.00 | 1.610 | .312 |
| 40.00 | 1.525 | .375 |
| 42.00 | 1.352 | .500 |
| 44.00 | 1.108 | .750 |
| 46.00 | .875 | 1.125 |
| 48.00 | .762 | 0 |

[1]Coordinates are defined in figure 1(b).

Model Characteristics:

| | |
|---|---|
| Basic configuration | Model A |
| Configuration with store | Model B |
| Configuration with cavity | Model C |
| Wing aspect ratio | 3.0 |
| Wing taper ratio | 0.2 |
| Wing mean aerodynamic chord ($\bar{c}$), ft | 1.293 |
| Free-stream airfoil | NACA 65A004 |
| Sweepback angle of quarter chord | 52.5° |
| Total wing planform area, sq ft | 3.802 |
| Total exposed fin area, sq ft | 1.332 |
| Fuselage fineness ratio | 10.0 |
| Fuselage frontal area, sq ft | 0.230 |
| Store fineness ratio | 8.0 |
| Store frontal area, sq ft | 0.058 |

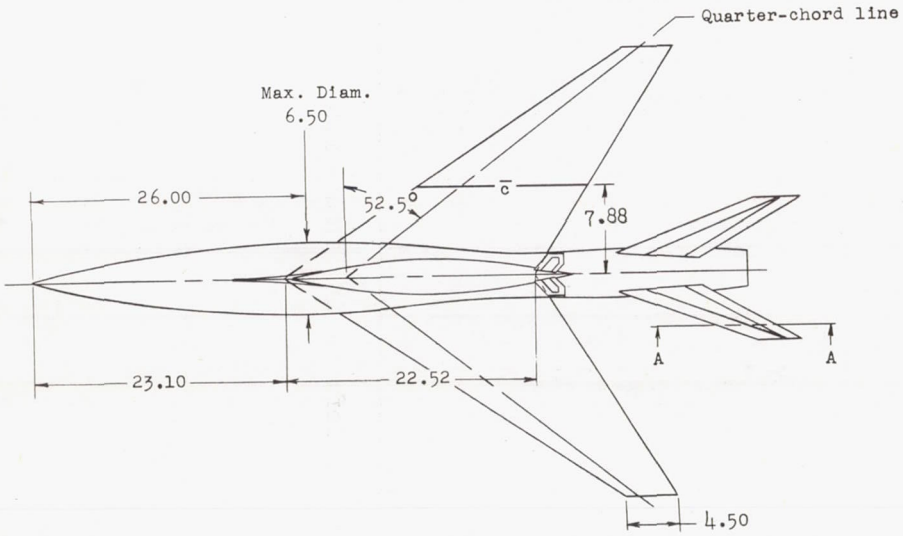


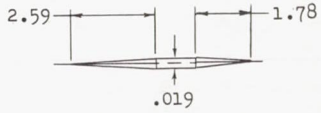


Section A-A

Typical fin section

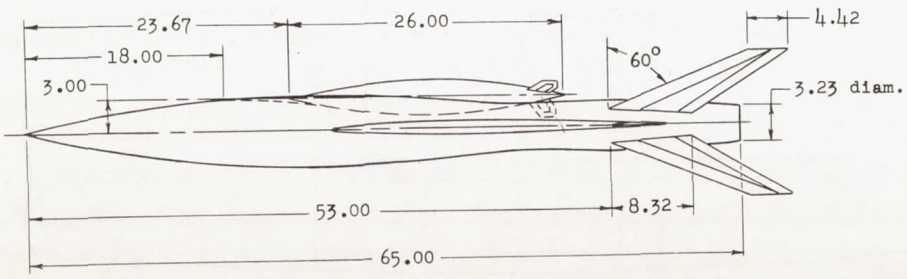


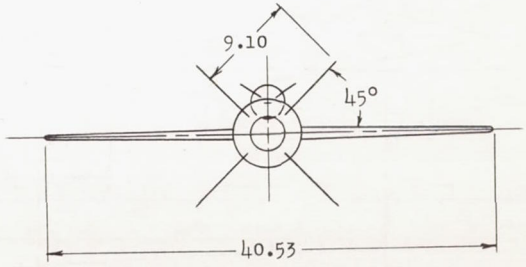


(a) Configuration with parabolic store and cavity.

Figure 1.- Details and dimensions of models tested. All dimensions are in inches.

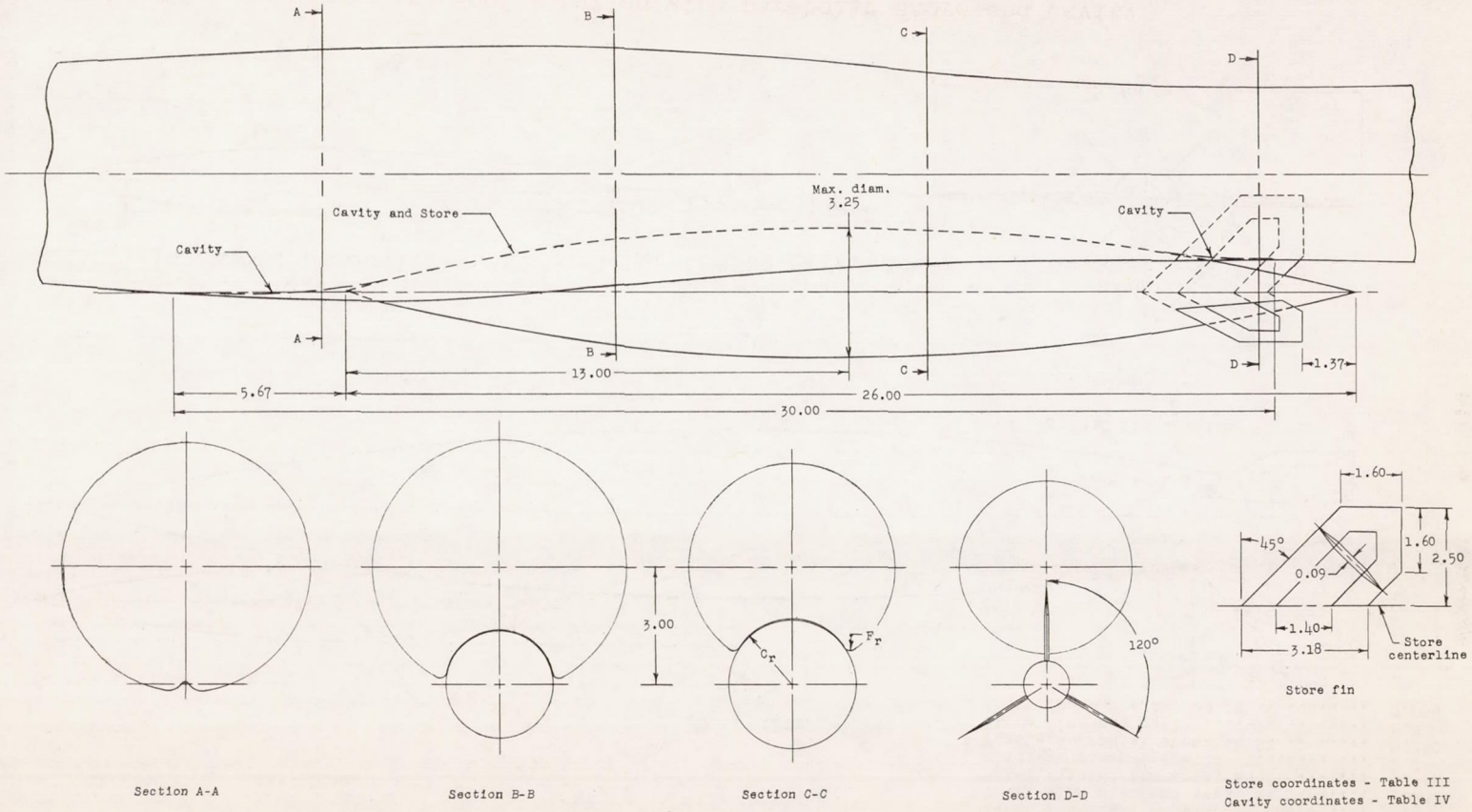


(b) Details of parabolic store and cavity.

Figure 1.- Continued.

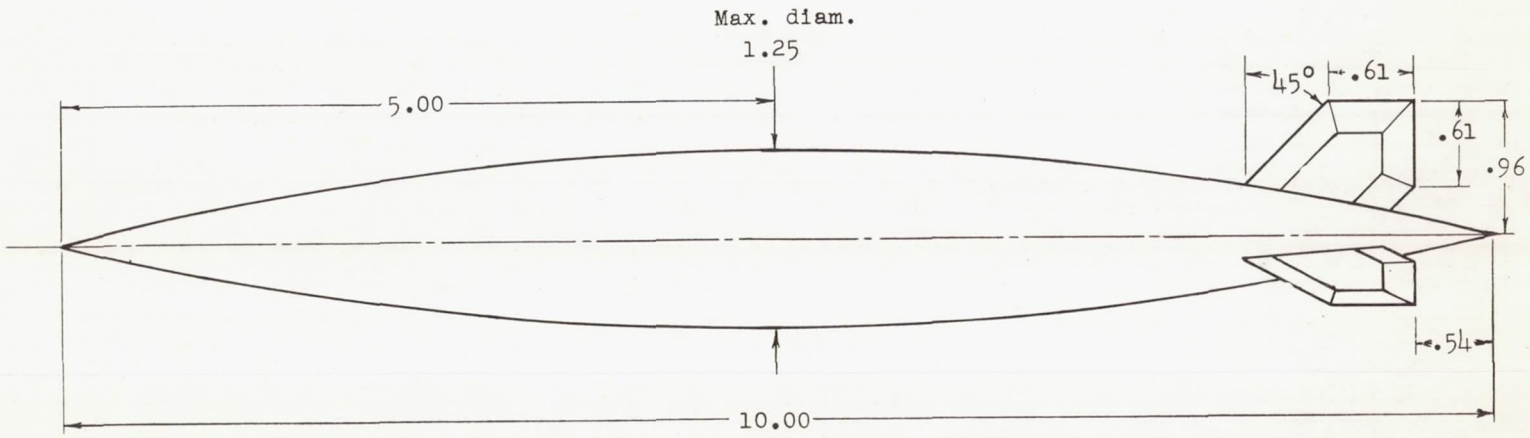


(c) Small parabolic store used for the interference-free drag test. Model E.

Figure 1.- Concluded.

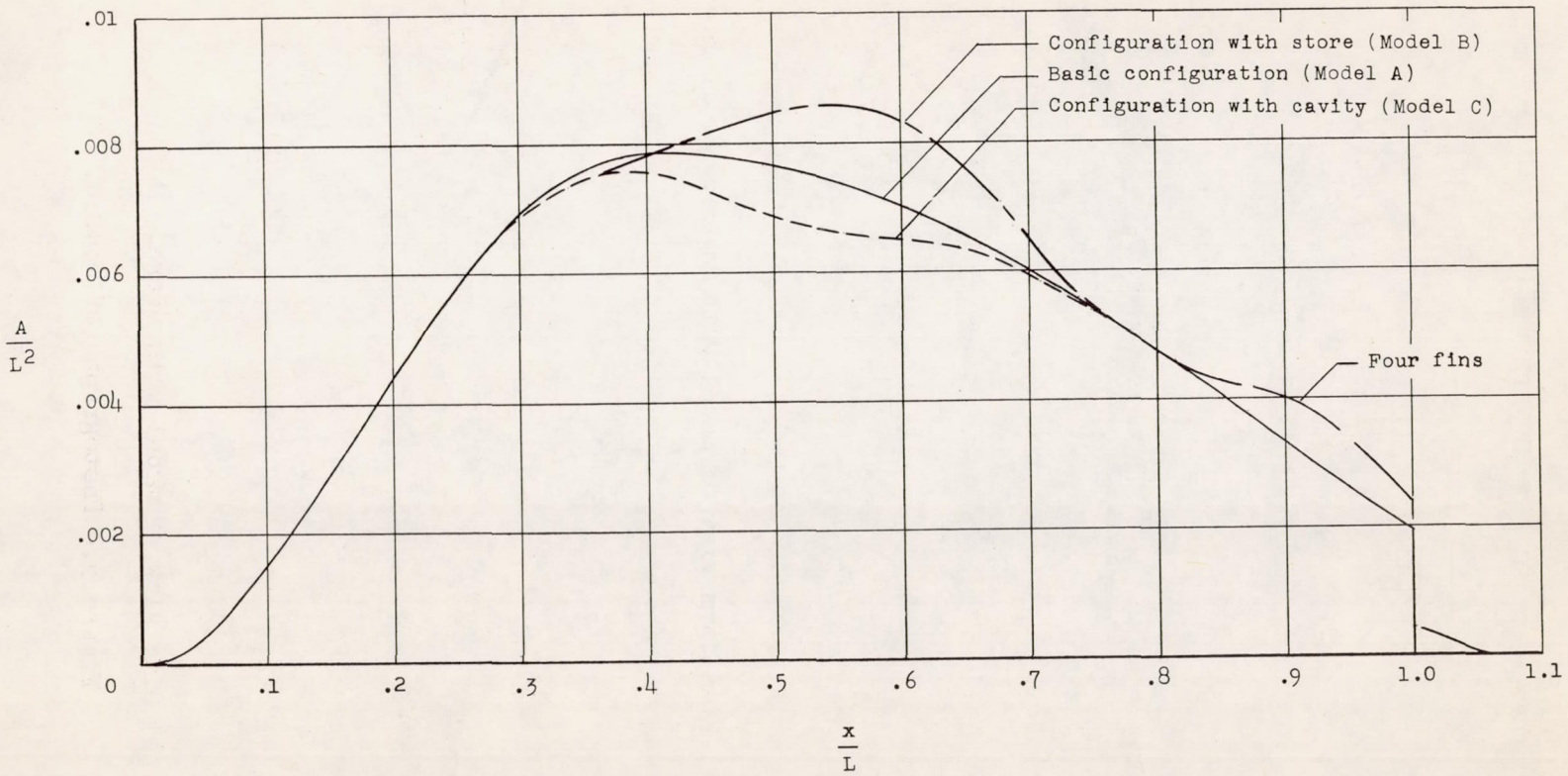


Figure 2.- Normal cross-sectional area distributions of configurations tested.

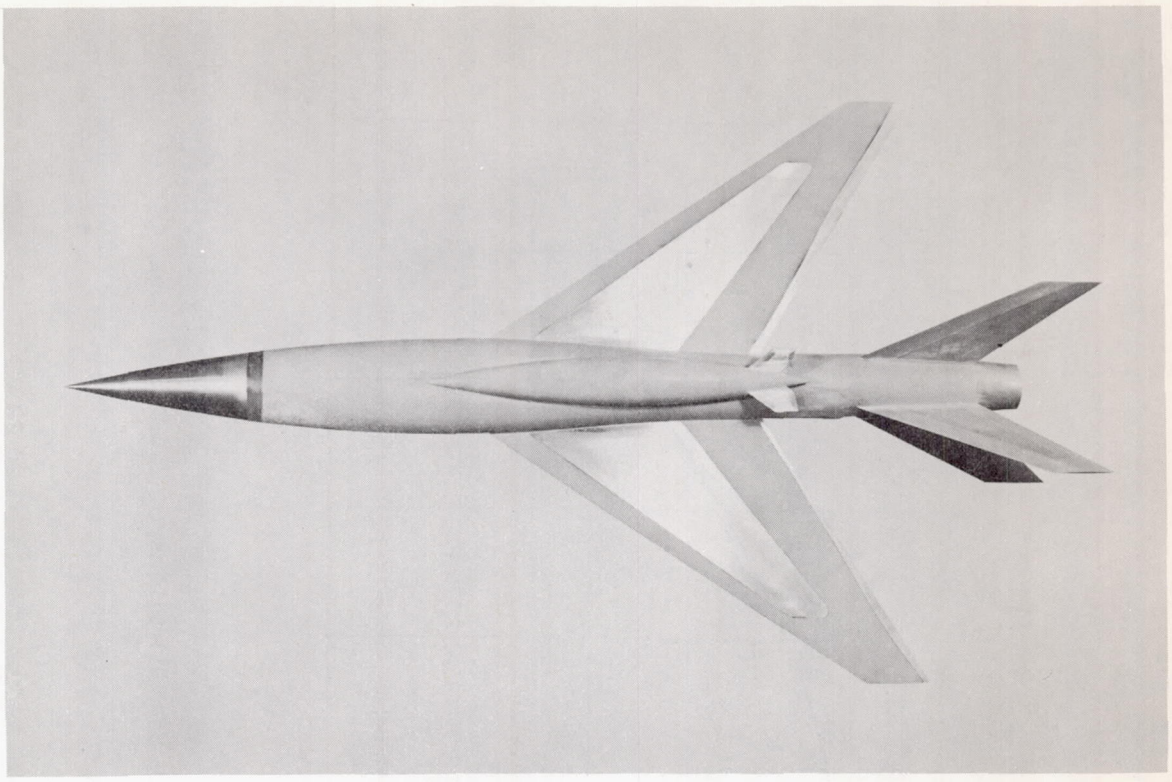

(a) Plan form view of model with store. Model B. L-90013.1

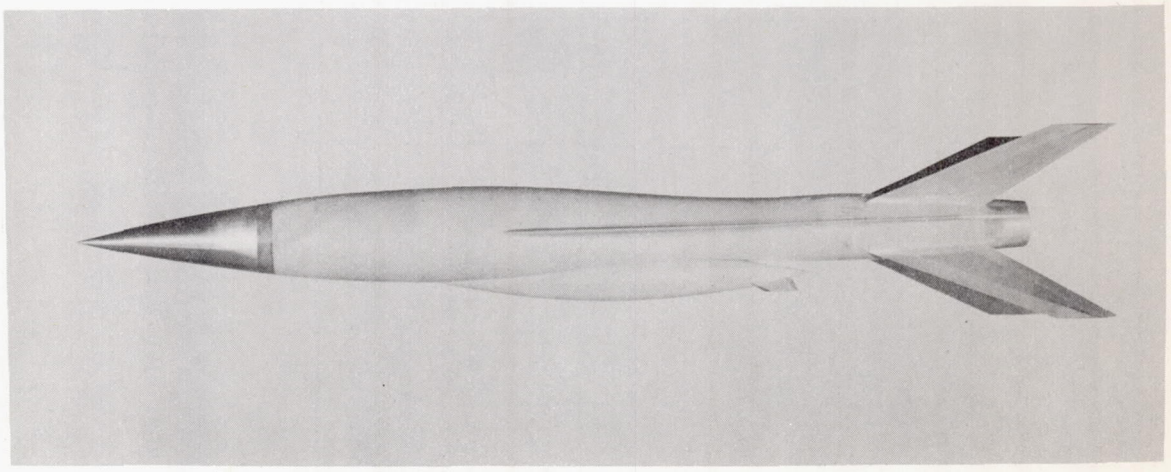

(b) Side view of model with store. Model B. L-90015.1

Figure 3.- Photographs of models.

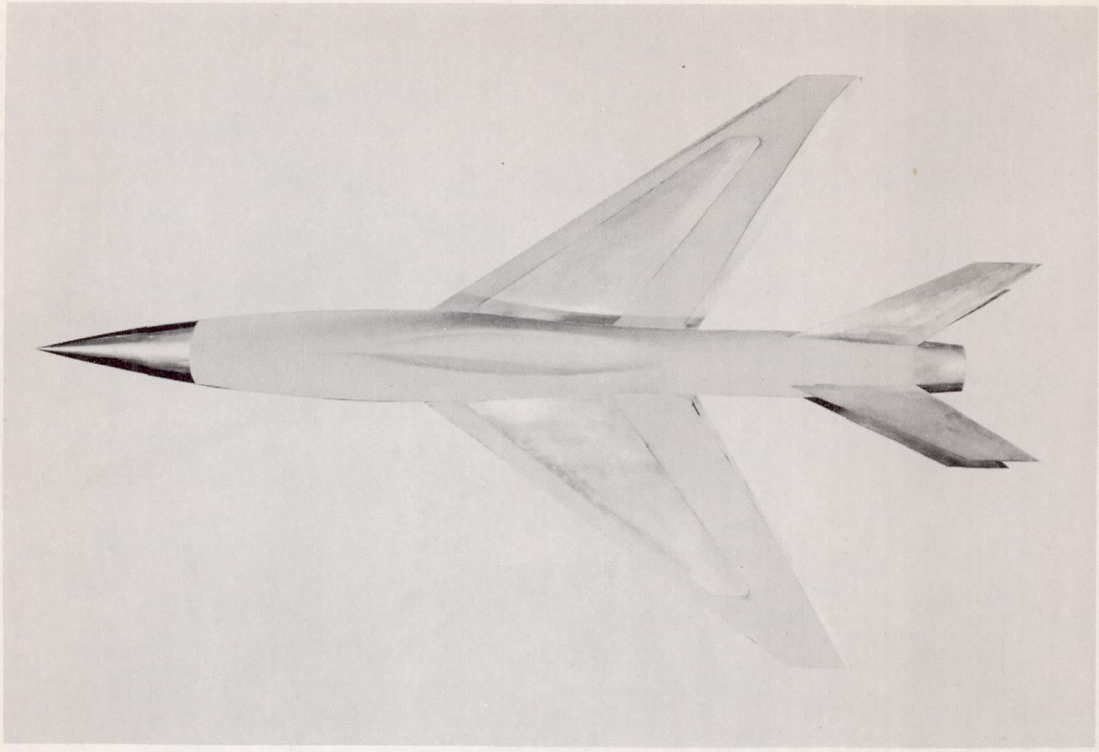

(c) Plan form view of model with cavity. Model C. L-89673.1

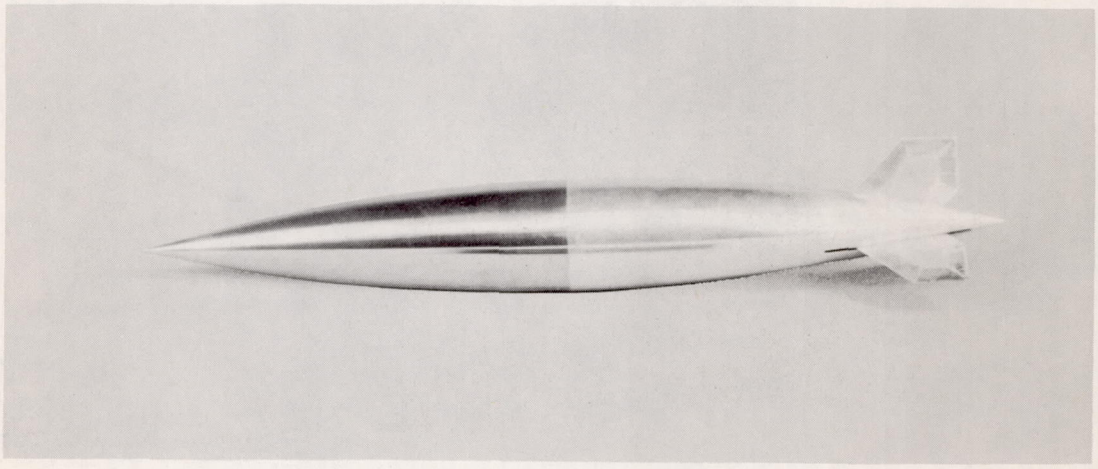

(d) Side view of small parabolic store. Model D. L-88041.1

Figure 3.- Continued.

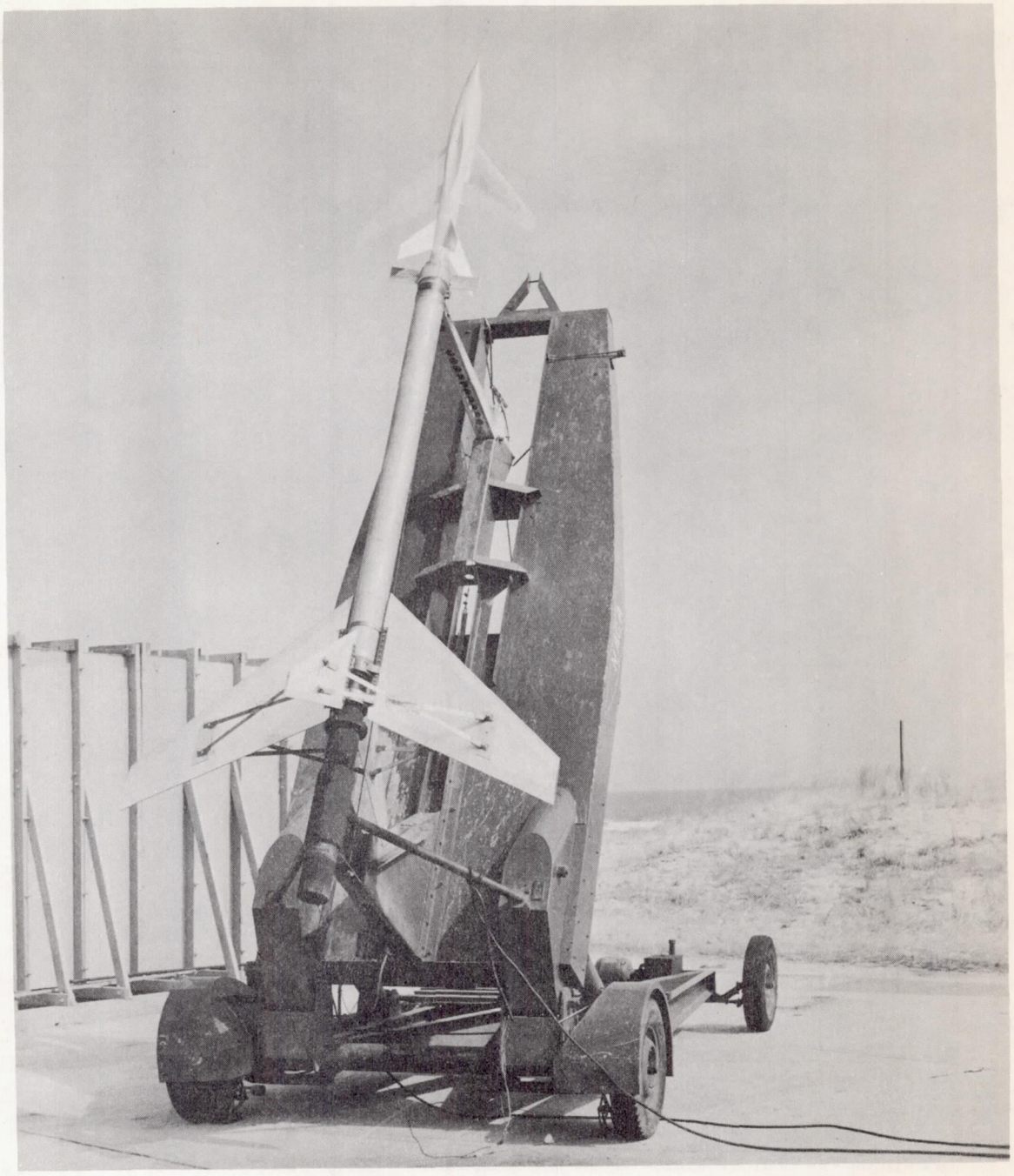

(e) Model C and booster on launcher. L-93450.1

Figure 3.- Concluded.

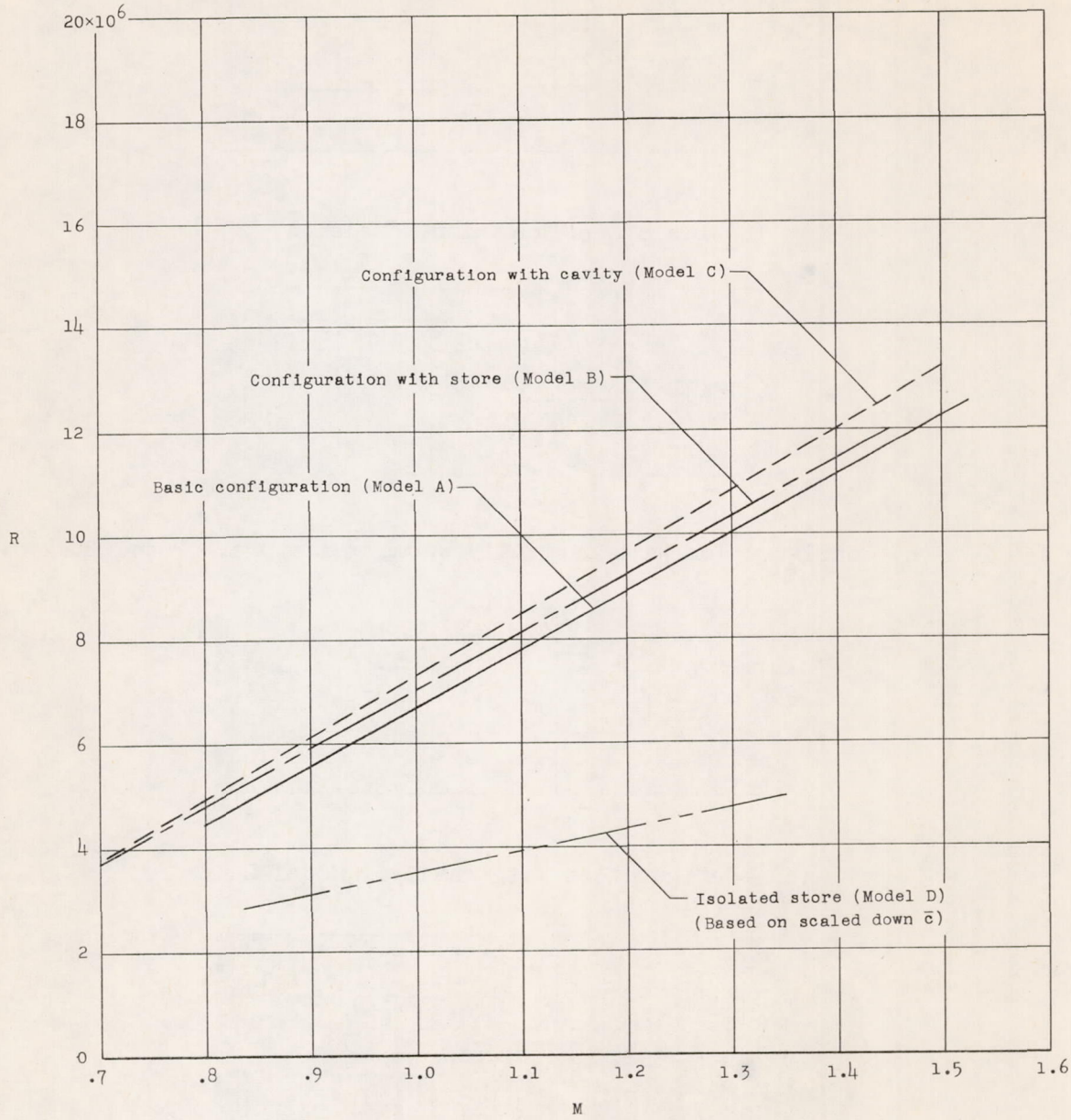


Figure 4.- Variations of Reynolds number with Mach number for models tested. Reynolds number is based on wing mean aerodynamic chord.

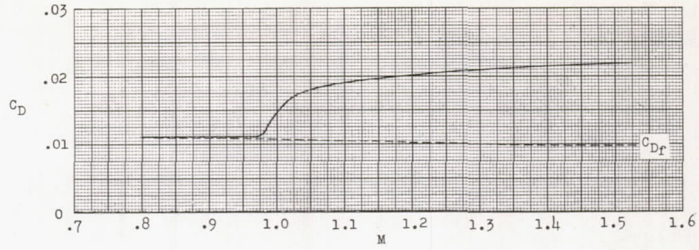


(a) Basic configuration. Model A.

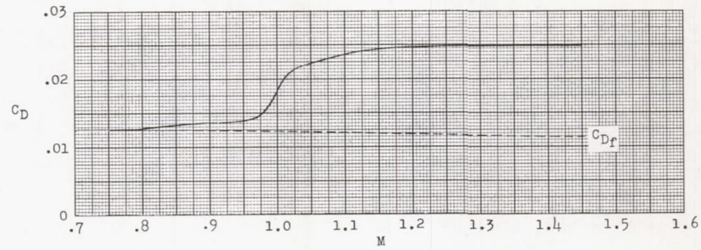


(b) Configuration with partially submerged store. Model B.

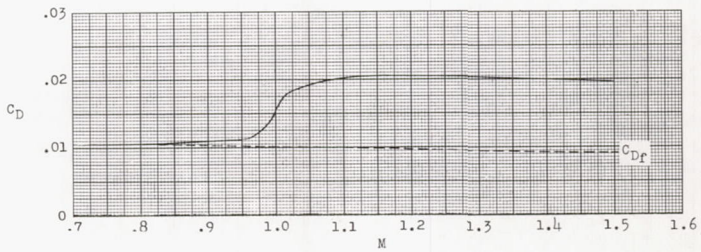


(c) Configuration with cavity. Model C.

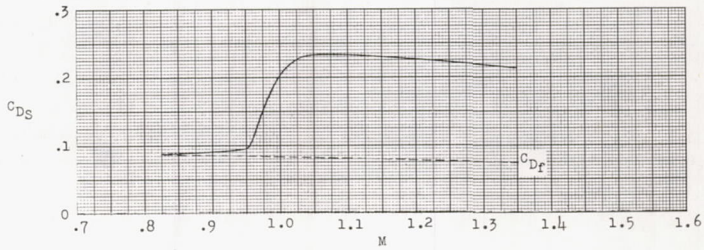


(d) Store. Model D.

Figure 5.- Variations of total drag and friction drag coefficients with Mach number for models tested.

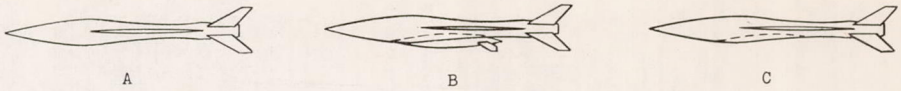


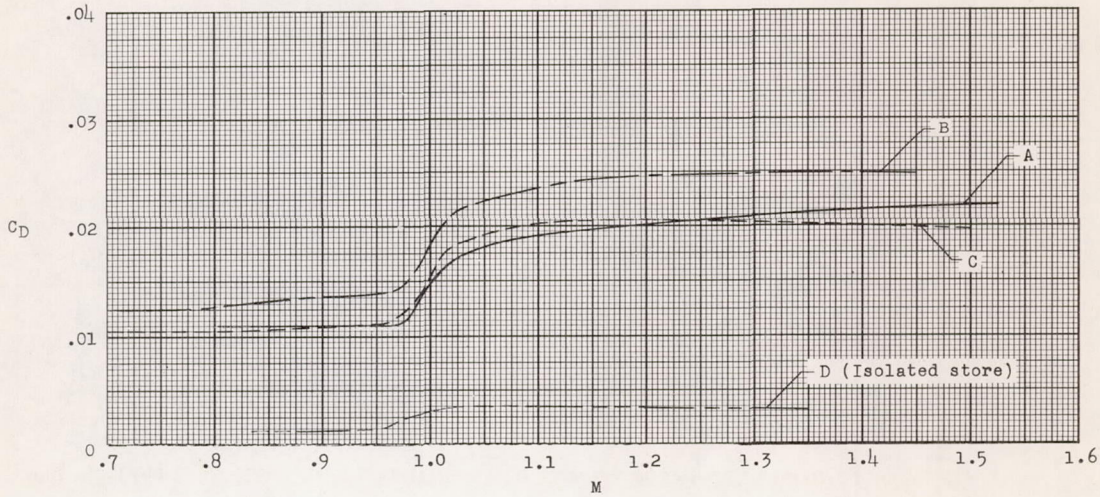


(a) Total drag.

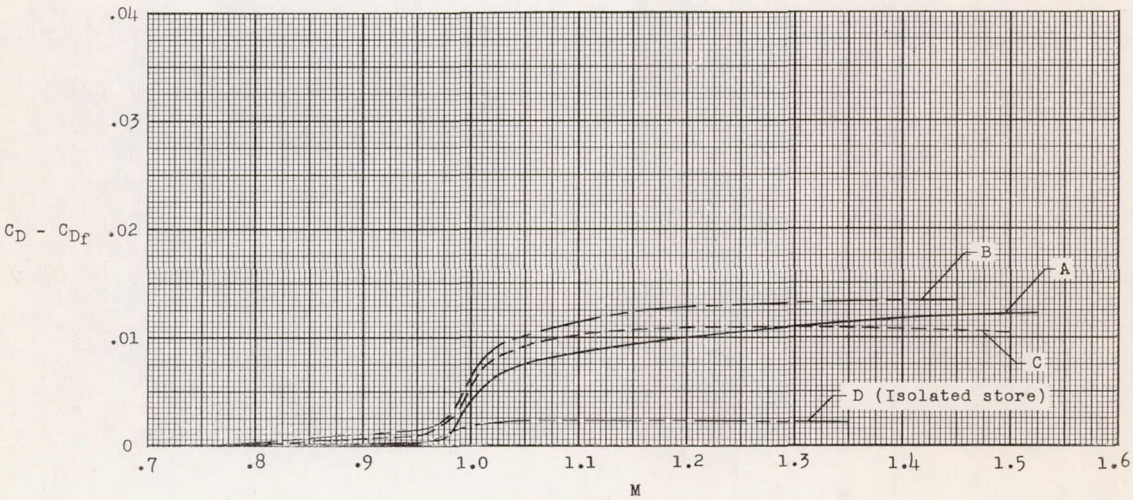


(b) Pressure drag.

Figure 6.- Comparisons of the total drag and pressure drag coefficients of the models tested.